Journal of Neuroscience Research 87:1474–1483 (2009)

Aluminum-induced Defective Mitochondrial Metabolism Perturbs Cytoskeletal Dynamics in Human Astrocytoma Cells

J. Lemire,[1] R. Mailloux,[1] S. Puiseux-Dao,[2] and V. D. Appanna[1]*

[1]Department of Chemistry and Biochemistry, Laurentian University, Sudbury, Ontario, Canada
[2]USM 505/EA 4105, Ecosystème et interactions toxiques, Département de regulations, development, et diversité moléculaire, Muséum Nationale d'Histoire Naturelle, Paris, France

Although aluminum (Al), a known environmental toxin, has been implicated in a variety of neurological disorders, the molecular mechanism responsible for these conditions is not fully understood. In this report, we demonstrate the ability of Al to trigger mitochondrial dysfunction and ineffective adenosine triphosphate (ATP) production. This situation severely affected cytoskeletal dynamics. Whereas the control cells had well-defined structures, the Al-exposed astrocytoma cells appeared as globular structures. Creatine kinase (CK) and profilin-2, two critical modulators of cellular morphology, were markedly diminished in the astrocytoma cells treated with Al. Antioxidants such as α-ketoglutarate and N-acetylcysteine mitigated the occurrence of the globular-shaped cells promoted by Al toxicity. Taken together, these data reveal an intricate link between ATP metabolism and astrocytic dysfunction and provide molecular insights into the pathogenesis of Al-induced neurological diseases.

Key words: aluminum; energy metabolism; ATP; creatine kinase; cytoskeletal dynamics; astrocytes

All life forms rely on adenosine triphosphate (ATP) as their universal energy currency in order to perform numerous cellular tasks. The energy harnessed from ATP is used to drive protein synthesis, DNA repair, ion transport, and the maintenance of cytoskeletal structure and dynamics (Wieser and Krumschnabel, 2001; Kovar et al., 2006). ATP can be generated in a number of ways, including during anaerobic respiration via substrate level phosphorylation and aerobic respiration via oxidative phosphorylation (Fink, 2002; Leach et al., 2002). In most aerobic organisms, the mitochondria house the necessary enzymatic machinery and respiratory complexes required to synthesize ATP in an O_2-dependent manner. While the tricarboxylic acid (TCA) cycle produces the necessary reducing equivalents, NADH and $FADH_2$, the respiratory complexes transfer the electrons from these moieties to the terminal electron acceptor, O_2. This process is coupled to the formation of a H^+ gradient, which is tapped to drive ATP formation (Yoshida et al., 2001). Complex eukaryotes also rely on other sources of ATP such as phosphogens in order to sustain energy demands (Sauer and Schlattner, 2004). Highly oxidative tissues such as the human brain and skeletal muscle invoke creatine kinase (CK) to produce ATP from phosphocreatine when energy is in high demand (Saks et al., 1996).

The brain consumes the most energy in the human body. Indeed, neurons rely on a steady supply of ATP in order to maintain cerebral functions. Astrocytes play a key role in supporting neuronal energy metabolism. These specialized cells also help in modulating synaptic firing and efficiency, supply trophic factors, and support the blood–brain barrier (Anderson and Swanson, 2000; Anderson and Nedergaard, 2003). The ability of astrocytes to perform these vital functions has been attributed to their unique morphology (Derouiche et al., 2002). Indeed, the specific arrangement of the actin and intermediate filaments provides the critical framework necessary to maintain a well-defined morphology that is required for the proper functioning of the astrocytes. The maintenance of this cytoskeletal configuration is inherently dependent on ATP. The polymerization of actin relies on a steady supply of ATP (Gourlay and Ayscough, 2005). Hence, energy metabolism, cytoskeletal structure, and neuronal function are intimately linked (Ames, 2000; Gartlon et al., 2006).

Environmental stressors and toxins, such as Al, are known to limit the aerobic production of ATP, a situation that may have a negative influence on astrocytic function. Al, a pro-oxidant, has also been shown to perturb the cytoskeleton in neurons and astrocytes (Aremu

*Correspondence to: V. D. Appanna, Department of Chemistry and Biochemistry, Laurentian University, Sudbury, Ontario, P3E 2C6, Canada. E-mail: VAppanna@laurentian.ca

Received 11 August 2008; Revised 8 October 2008; Accepted 10 October 2008

Published online 15 December 2008 in Wiley InterScience (www.interscience.wiley.com). DOI: 10.1002/jnr.21965

and Meshitsuka, 2006). In fact, the loss of cytoskeletal dynamics and astrocyte morphology has been associated with the pathogenesis of Alzheimer's disease (Ting et al., 2007). However, the molecular details underlying the Al-mediated perturbation of the cytoskeleton in astrocytes remain poorly understood. In this study, we report on how the Al-mediated disruption of astrocyte morphology is a manifestation of dysfunctional energy metabolism. The diminution in the production of ATP coupled with ineffective CK contributes to the abnormal morphology observed in the Al-stressed astrocytes. The intricate relationship involving Al toxicity, defective ATP production, cellular morphology, and neurological disease is discussed.

MATERIALS AND METHODS

Culturing and Isolation of CCF-STTG1 Cells

The human astrocytoma cell line (CCF-STTG1) was acquired from the ATCC (Manassas, VA). The efficacy of this cell line stems from its maintenance of normal astrocytic properties (Mentz et al., 1999). The astrocytic cell line was cultured as described by Lemire et al. (2008). The media [α-minimal essential medium (MEM)] either included fetal bovine serum (FBS) or was devoid of FBS (5 mM D-glucose is present in α-MEM). Upon reaching 75% confluence, the cell monolayer was washed with phosphate-buffered saline (PBS; 136 mM sodium chloride, 2.5 mM potassium chloride, 1.83 mM dibasic sodium phosphate, and 0.43 mM monobasic potassium phosphate, pH 7.4) and then resupplemented with serum-free media containing 2.5 mM lactate chelated to varying amounts of Al (0.01–0.1 mM) or 2.5 mM lactate with 40 μM H_2O_2. Cells exposed to lactate (2.5 mM) alone served as the control. For recovery experiments, after a 24-hr stressing period, the cells were incubated with serum-free media reconstituted with N-acetylcysteine (NAC) or 5 mM α-ketoglutarate (KG) for 24 hr. Cells were fractionated into mitochondrial and cytoplasmic portions as described by Lemire et al. (2008). Purity of fractions was deduced by detecting the levels of voltage-dependent anion channel (VDAC) (mitochondria) and F-actin (cytosol). Protein content was analyzed by the Bradford assay with bovine serum albumin used as the standard (Bradford, 1976).

Fluorescence Microscopy

To visualize the impact of Al and H_2O_2 on astrocytic morphology, immunofluorescence microscopy was used. CCF-STTG1 cells were grown to a minimal density on coverslips and exposed to control, Al, and H_2O_2 conditions. The coverslips were washed with 0.5 mM EDTA and PBS and prepared for microscopic examination (Lemire et al., 2008). Primary analysis of cellular morphology was ascertained by phase contrast microscopy with a Nikon confocal microscope at 20× ocular magnification. For visualization of the actin framework, the slides were stained with phalloidin (1.5 mg/ml) conjugated with either fluorescein isothiocyanate (FITC) or rhodamine B for 20 min. For the detection of reactive oxygen species (ROS) levels within the astrocytes, the cells were incubated with 20 μM of dicholorodihydrofluorescein diacetate (DCFH-DA) in α-MEM and 10% FBS for 1 hr at 37°C. The nucleus was identified by Hoechst 33528 (2.5 μg/ml in PBS). The status of intermediate filaments was made apparent by incubating cells in a cyanine III (Cy3)-conjugated glial fibrillary acidic protein (GFAP) primary antibody (Sigma). The coverslip was submerged in Tween-20–Tris-buffered saline (TTBS) with 5% FBS for 1 hr to block nonspecific binding sites. The coverslip was then rinsed three times with Tris-buffered saline (TBS). The Cy3-GFAP (1/800) in TBS/5% FBS solution was then introduced for a period of 45 min. Similar procedures were used for the detection of CK-brain isoform (CK-BB) and profilin-2. The primary antibodies (1:800) were obtained from Abcam. The coverslips were then washed thoroughly with TBS and incubated with anti-mouse (CK) and anti-rabbit (profilin-2) conjugated to FITC (Santa Cruz). The cells were subsequently visualized with an inverted deconvolution microscope (Zeiss).

Blue Native–Polyacrylamide Gel Electrophoresis (BN-PAGE) and In-gel Activity Assays

BN-PAGE was performed as described in (Mailloux et al., 2007; Schagger and von Jagow, 1991). Gradient gels (4–16%) were favored for these assays. Briefly, 2 μg of protein equivalent per microliter was prepared in blue native buffer (500 mM 6-amino hexanoic acid, 50 mM BisTris [pH 7.0], and 1% dodecyl-β-D-maltoside). For soluble proteins, dodecyl-β-D-maltoside was omitted. Each well of the native gel was loaded with 30 μg of prepared protein samples. Once the electrophoresis was completed, the native gel was incubated in equilibration buffer (25 mM Tris-HCl, 5 mM $MgCl_2$ [pH 7.4]) for 15 min. In-gel activity was ascertained by using a reaction mixture containing equilibration buffer, 5 mM substrate, 0.5 mM cofactor, 0.5 mg/ml iodonitrotetrazolium chloride, and 0.2 mg/ml phenazine methosulfate. For the activity detection of NAD-dependent isocitrate dehydrogenase (NAD-ICDH), 5 mM isocitrate, and 0.5 mM nicotinamide adenine dinucleotide (NAD) was used. Similarly, malate dehydrogenase was detected by the addition of 5 mM malate and 0.5 mM NAD. Activity of nucleotide diphosphate kinase (NDPK) was established by the addition of 1 mM ADP (adenosine 5′-diphosphate), 1 mM guanosine triphosphate (GTP), 15 mM glucose, 5 units of hexokinase, 5 units of glucose-6-phosphate dehydrogenase, and 1 mM NADP (Mailloux et al., 2008). CK activity was monitored with a reaction mixture similar to NDPK except 5 mM phosphocreatine (PCr) replaced GTP. Enzymatic activity of cytochrome *c* oxidase (Cyt *c* Ox) was visualized by the addition of a reaction mixture consisting of equilibration buffer supplemented with 5 mM KCN, 5 mg/ml of diaminobenzidine, 562.5 mg/ml of sucrose, and 10 mg/ml of cytochrome *c* (Mailloux et al., 2007b).

Immunoblot Analysis

Sodium dodecyl sulfate (SDS)-PAGE and 2D SDS-PAGE was performed with the modified method previously described (Laemmli, 1970; Lemire et al., 2008). The proteins were solubilized in 62.5 mM Tris-HCl (pH 6.8), 2% SDS, and 2% β-mercaptoethanol at 100°C for 5 min and electro-

phoresed on a 10% isocratic denaturing gel. 2D immunoblot analysis was performed as previously described (Lemire et al., 2008). After electrophoresis, the proteins were blotted on to a Hybond-polyvinylidene diflouride membrane for immunoblotting. Nonspecific binding sites on the membrane were blocked by treatment with 5% nonfat skim milk dissolved in TTBS (20 mM Tris-HCl, 0.8% NaCl, 1% Tween-20 [pH7.6]) for 1 hr. Secondary antibodies (Bio-Rad) consisted of horseradish peroxidase–conjugated goat anti-mouse (profilin-2) and goat anti-rabbit (CK). The detection relied on incubation of the probed membrane for 5 min at room temperature in the presence of Chemiglow reagent (Alpha Innotech). Visualization of the immunoblot was documented via a ChemiDoc XRS system (Bio-Rad Imaging Systems).

Metabolite Analysis

To monitor the cellular levels of ATP, creatine (Cr), and PCr, cells were treated with 1% perchloric acid and then analyzed by high-performance liquid chromatography (HPLC). Samples were injected into a C_{18}-reverse phase column (Phenomenex) operating at a flow rate of 0.7 ml/min. The mobile phase consisted of 20 mM KH_2PO_4 (pH 2.9 with 6N HCl). The identities of the metabolites were compared with known standards, and the metabolite mixtures were spiked with the given metabolites to confirm peak retention times.

Statistical Analysis

All experiments were performed three times and in duplicate. Where appropriate, the Student *t*-test was used to assess significance.

RESULTS

Al Perturbs the Cytoskeleton in Astrocytoma Cells

To determine the impact of Al on the organization of the cytoskeleton, we investigated the cellular distribution of GFAP and actin by immunofluorescence microscopy. In control cells, the GFAP and actin were organized in a filamentous pattern. Exposure to concentrations of Al as low as 0.01 mM resulted in the disruption of the polymerized structure of actin and GFAP. Because Al is well known for its pro-oxidant properties, the impact of H_2O_2, a ROS-producing molecule, on the cytoskeletal framework was investigated. A 24-hr exposure to 40 μM H_2O_2 also resulted in the perturbation of the GFAP and actin cytoskeletal arrangements (Fig. 1, III). These structural changes were clearly evident in the phase contrast micrographs. The microscopic images at higher magnification revealed the filamentous nature of the actin arrangement in the control cells as opposed to globular actin structure in the Al-treated cells (Fig. 1, I, II, III). In order to account for the Al-mediated disruption of the cytoskeleton, the levels of the apoptotic markers in the cytosol, cytochrome *c*, and cleaved caspase-3 were probed. Cytochrome *c* and cleaved caspase-3 were not detected in the cytosol, thus indicating that apoptosis was not contributing significantly to the Al-mediated disruption of the cytoskeleton (data not shown).

Al Toxicity Perturbs Aerobic ATP Production

Because the maintenance of cytoskeletal structure and function relies on a steady supply of ATP, we probed the impact of Al on aerobic respiration. The activity of Cyt *c* Ox, a respiratory complex required for the transfer of electrons to the terminal electron acceptor oxygen, displayed a sharp decrease in activity in the mitochondria from the Al-treated cells (Fig. 2, I). H_2O_2 had a similar effect on Cyt *c* Ox. The negative impact of Al on the aerobic ATP-producing machinery was confirmed by testing the activity of NAD-ICDH. In contrast to the Al-exposed cells, a more intense activity band was recorded in the mitochondria from the control cells (Fig. 2, II). Other TCA cycle enzymes such as α-ketoglutarate dehydrogenase and succinate dehydrogenase also displayed a marked decline in activity after Al exposure (data not shown). HPLC analysis of the total cellular ATP levels provided further insight into the impact of Al on mitochondrial metabolism. Indeed, a significant decrease in cellular ATP levels was recorded in the Al-treated cells (Fig. 2, III). To probe the influence of Al on cellular energetics further, we tested the activity NDPK by BN-PAGE. NDPK plays a crucial role in maintaining ADP availability for aerobic respiration (Dzeja and Terzic, 2003). The activity of NDPK was diminished in the Al-exposed cells (Fig. 2, IV). However, it is important to note that malate dehydrogenase, another key mitochondrial enzyme, was not diminished in the stressed conditions (Fig. 2, V). This clearly illustrates that Al toxicity was affecting the molecular functioning of the mitochondria.

CK Is Perturbed in the Al-treated Cells

Because Al affected aerobic respiration and cellular ATP levels, we tested other enzymes involved in the maintenance of the cellular energy budget. CK is an excellent candidate because this enzyme produces ATP from PCr when energy is in high demand. Whereas an intense activity band was recorded in the control cytosol, the formazan precipitate was absent in the Al-stressed cells (Fig. 3, I). Two-dimensional silver staining and immunoblot of the activity bands revealed that a drastic decrease in activity in the Al-exposed cells (Fig. 3, II and III). HPLC analysis of Cr and PCr levels also pointed to the Al-mediated disruption of CK. In contrast to control cells, the Al- and H_2O_2-treated cells contained less Cr and PCr (Fig. 3, IV). These data suggest that biosynthesis of Cr and its subsequent use for ATP formation were perturbed. The CK protein levels and the cellular localization of this enzyme were examined by immunofluorescence microscopy. Cells exposed to 0.1–0.01 mM Al and 40 μM H_2O_2 contained less CK than their control counterparts (Fig. 4). The presence of either Al or H_2O_2 also disrupted the cellular localization of CK. Indeed, although CK was associated with the actin filaments in the control cells, this phosphagen-producing enzyme seemed to be predominantly clustered around the nucleus in the Al- and H_2O_2-exposed cells. Thus, Al appears to perturb the cellular energy budget by interfering with aerobic respiration and CK.

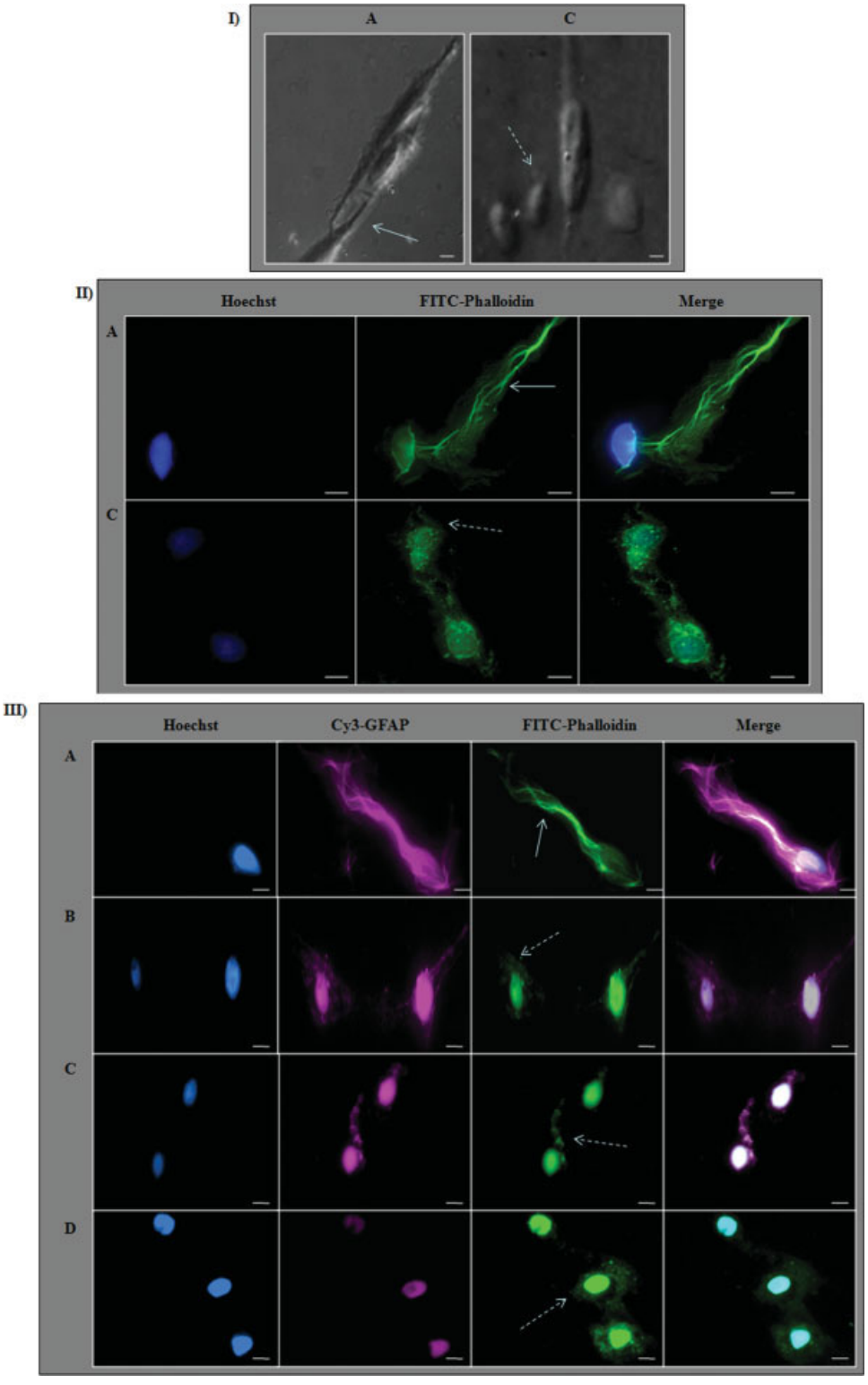

Fig. 1. Microscopic studies of human astrocytoma cells. **A:** Control cells. **B:** Cells exposed to 0.01 mM Al. **C:** Cells exposed to 0.1 mM Al. **D:** Cells exposed to 40 μM H_2O_2 for 24 hr. **I:** Phase contrast microscopic images. Microscopy was performed at 20× ocular objective. **II:** Astrocytoma stained with Hoechst 33528 (nucleus) and FITC-phalloidin (actin). Microscopy was performed at 60× ocular objective. **III:** After treatment, cells were stained with Hoechst 33528 (nucleus), Cy3-GFAP, and FITC-phalloidin (actin). Microscopy was performed at 40× ocular objective; scale bar = 10 μm. Solid arrows indicate well-defined structures; broken arrows, changes in the stressed cells. [Color figure can be viewed in the online issue, which is available at www.interscience.wiley.com.]

Profilin-2 Is Diminished in Al-exposed Astrocytoma Cells

The loss of the filamentous pattern of the cytoskeleton and the perturbation of the cellular energy budget prompted us to assess the cellular levels of profilin-2. This protein plays a key role in recharging ADP-actin monomers with ATP for their subsequent addition to the barbed ends of the actin filaments (Kovar et al.,

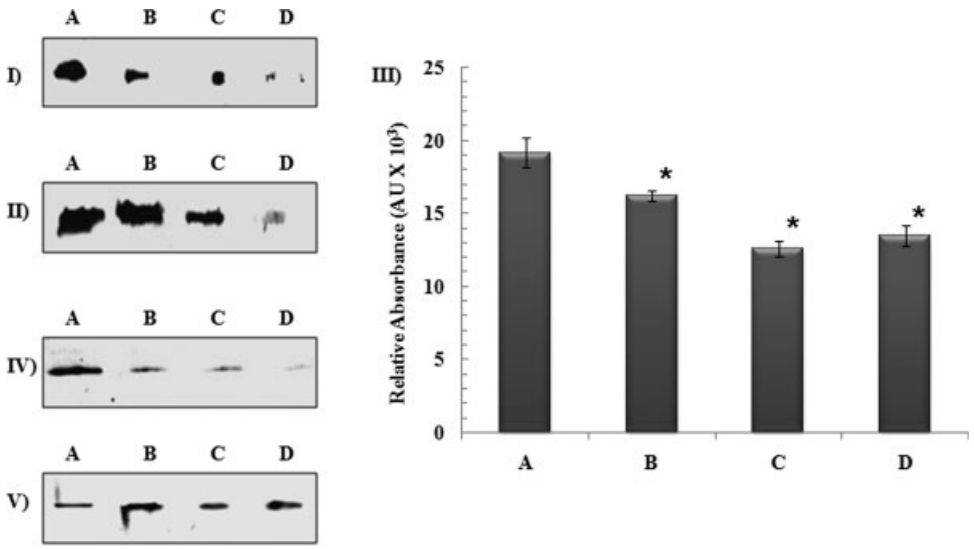

Fig. 2. Energy status of stressed human astrocytoma cells. Cells were incubated in (**A**) control, (**B**) 0.01 mM Al, (**C**) 0.1 mM Al, and (**D**) 40 μM H_2O_2 for 24 hr. **I:** In-gel activity stain for Cyt *c* Ox. **II:** In-gel activity stain for NAD-ICDH. **III:** HPLC analysis of cellular ATP levels. $n = 3 \pm$ SD; $P \leq 0.05$. ⋆Significant decrease of ATP compared with control treatment. **IV:** In-gel activity stain for NDPK. **V:** In-gel activity stain for malate dehydrogenase.

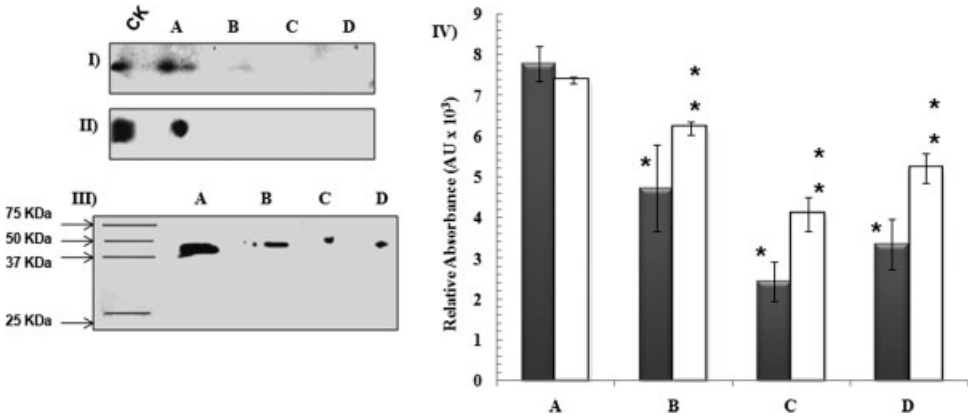

Fig. 3. Activity and expression of CK in astrocytoma cells under Al insult. CCF-STTG1 cells were incubated in (**A**) control, (**B**) 0.01 mM Al, (**C**) 0.1 mM Al, and (**D**) 40 μM H_2O_2 for 24 hr. **I:** In-gel activity stain for CK. **II:** Bands were excised from activity gel (I) and subsequently ran on a 10% SDS-PAGE gel and silver-stained for protein expression. A total of 10 μg of a CK standard was run in tandem with both experiments (sigma). **III:** Immunoblot assay for the brain isoform of CK. **IV:** Cr (solid bar) and PCr (open bar) levels were measured with a Waters HPLC with a C_{18}-reverse phase column. $n = 3 \pm$ SD; $P \leq 0.05$. ⋆Significant decrease in Cr levels compared with control treatment. ⋆⋆Significant decrease in PCr levels compared with control treatment. Activity bands were observed in the stressed conditions only after prolonged incubation periods.

2006). Immunoblot analysis revealed that the treatment of human astrocytoma cells with 0.01–0.1 mM Al or H_2O_2 abolished profilin-2 levels relative to control (Fig. 5). Immunofluorescence microscopy revealed that the exposure of the cells to Al concentrations as low as 0.01 mM severely perturbed the amount and distribution of profilin-2. Whereas profilin-2 was uniformly distributed along the actin filaments throughout the control cells, this globular actin-binding protein appeared to be centralized around the nucleus of Al- and H_2O_2-exposed cells (Fig. 6). It is important to note that even though the levels of actin did not change significantly, in the stressed cells, its architecture was drastically perturbed.

NAC Treatment Restores the Cytoskeleton in Al-exposed Cells

DCFH-DA staining and fluorescence microscopy pointed to the increased amount of ROS in astrocytoma cells exposed to Al (Fig. 7, I). Indeed, concentrations of Al as low as 0.01 mM provoked ROS formation in these cells. In order to determine whether antioxidant treatment can reverse the toxic effects of Al, cells were incubated in NAC, a powerful antioxidant. A marked decrease in ROS levels was observed after NAC treatment (Fig. 7, II). Exposure to NAC partially recovered the filamentous pattern of actin and GFAP in the Al-treated cells. Similar effects were observed when H_2O_2-challenged cells were exposed to NAC for 24 hr (Fig. 8,

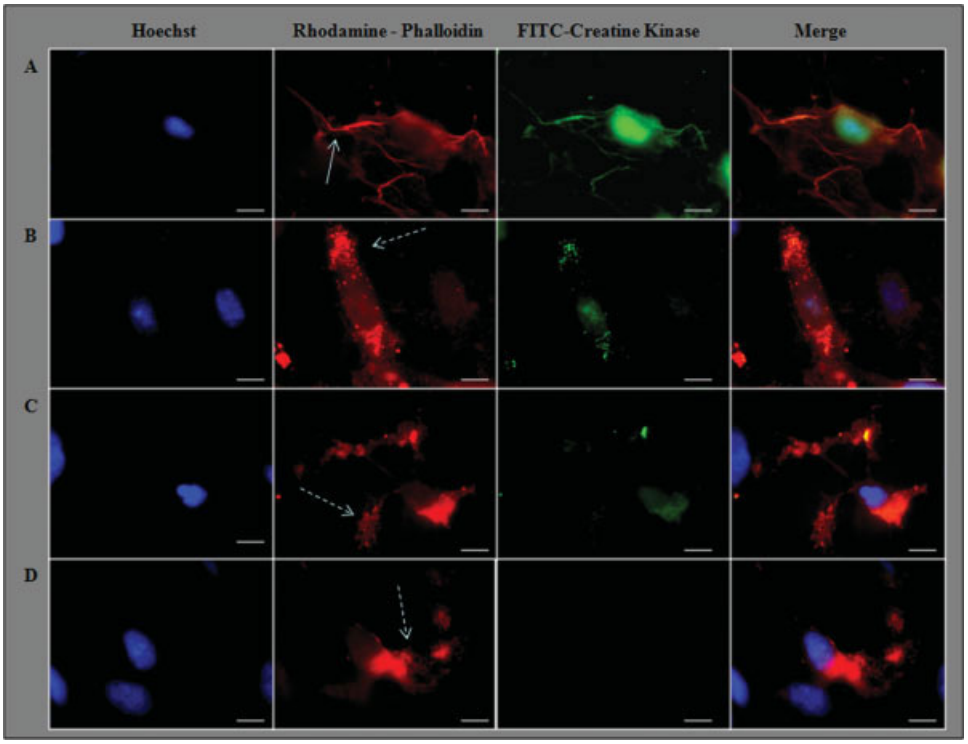

Fig. 4. CK and the actin cytoskeleton in astrocytoma cells incubated in (**A**) control, (**B**) 0.01 mM Al, (**C**) 0.1 mM Al, and (**D**) 40 μM H_2O_2 media for 24 hr. The cells were subsequently stained with Hoechst 33528 (nucleus), rhodamine-phalloidin (actin), and FITC-CK. The yellow demarcates the association of CK with the actin filaments. Microscopy was performed at 60× ocular objective; scale bar = 10 μm. Solid arrows indicate filamentous structure of actin (control conditions); broken arrows, loss of filamentous actin (stressed conditions). [Color figure can be viewed in the online issue, which is available at www.interscience.wiley.com.]

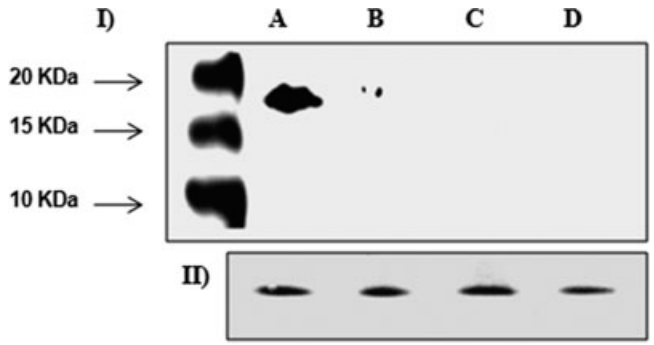

Fig. 5. Analysis of profilin-2 levels. Astrocytoma cells were incubated in (**A**) control, (**B**) 0.01 mM Al, (**C**) 0.1 mM Al, and (**D**) 40 μM H_2O_2 media for 24 hr. **I:** Immunoblot for profilin-2. **II:** Immunoblot for F-actin as a loading control. Although the actin levels are similar, in the stressed conditions, the structural features were markedly altered.

I). Furthermore, the exposure of Al and H_2O_2-treated cells to NAC increased the cellular levels of ATP (Fig. 8, II) relative to the untreated cells (Fig. 2, III). KG did mitigate the toxic influence of Al and H_2O_2 (data not shown).

DISCUSSION

Al toxicity has been linked to the pathogenesis of various disorders, including Alzheimer's disease, Parkinson's disease, obesity, and anemia (Becaria et al., 2002; Mailloux et al., 2007a). In this study, the exposure of human astrocytoma cells to Al resulted in increased ROS levels and dysfunctional mitochondrial metabolism. The Al-mediated disruption of the TCA cycle and electron transport chain (ETC) led to a sharp diminution in cellular ATP production. We have previously observed that Al severely compromises aerobic metabolism (Mailloux et al., 2007b; Singh et al., 2007). The inability to maintain cellular ATP levels as a consequence of Al can spell disaster for any cell. Indeed, this moiety is required to drive various cellular functions, including the maintenance of cytoskeletal structure and cell morphology (Pessoa-Pureur and Wajner, 2007). The cytoskeleton plays a crucial role in allowing these cells to support brain functions (Rutka et al., 1997; Pekny and Nilsson, 2005). Thus, the loss of morphology would have disastrous consequences in the human brain. In fact, perturbed astrocyte morphology has been characterized in various neurological diseases (Pekny and Nilsson, 2005).

In this study, the Al-mediated perturbation of mitochondrial metabolism in the astrocytoma cells and the concomitant reduction in cellular ATP levels had a dramatic effect on cytoskeletal structure and cell morphology. Al-exposed cells were not characterized by the activation of apoptosis; it appears that this process may not be prominent in this instance. Al has previously been shown to mediate cytoskeletal disassembly by apoptosis (Suarez-Fernandez et al., 1999). However, in this study, low levels of Al were used. The ability of NAC to recover the filamentous structure of the cytoskeleton and cellular ATP levels after Al treatment would further

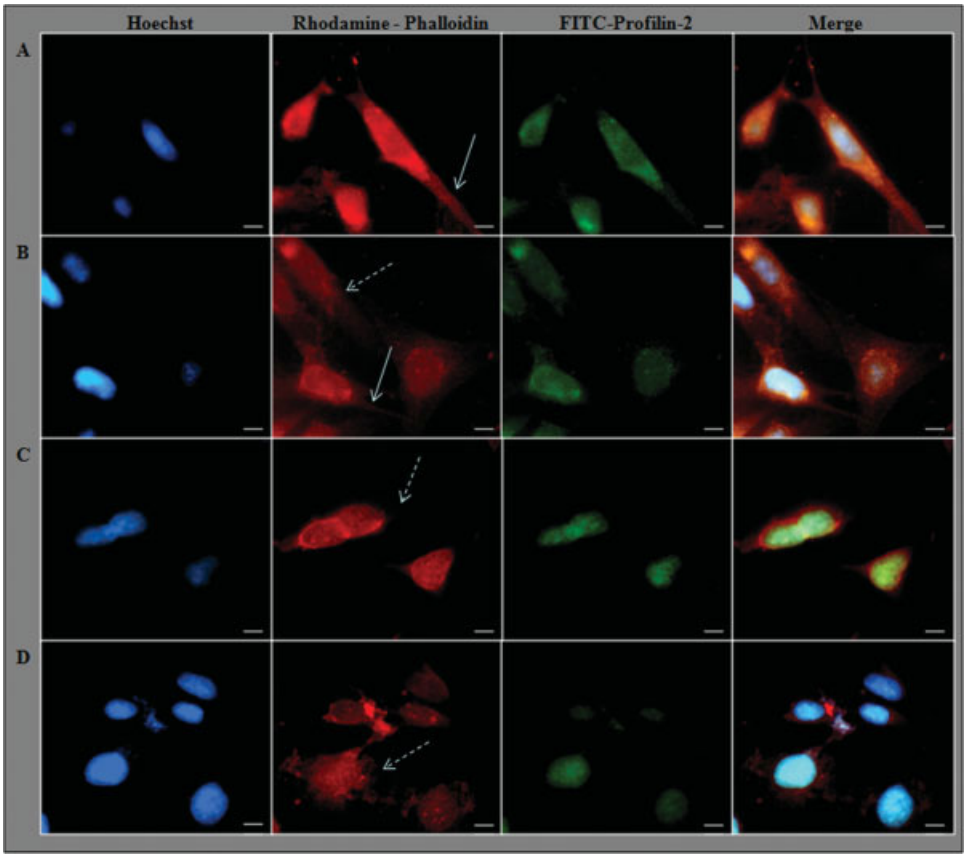

Fig. 6. Al-induced cytoskeletal dysregulation and profilin-2 expression. Astrocytoma were incubated in (**A**) control, (**B**) 0.01 mM Al, (**C**) 0.1 mM Al, and (**D**) 40 μM H_2O_2 for 24 hr. The cells were stained with Hoechst 33528 (nucleus), rhodamine-phalloidin (actin), and FITC-profilin-2. Yellow demarcates the association of profilin-2 with the actin filaments. Microscopy was performed at 40× ocular objective; scale bar = 10 μm. Solid arrows indicate filamentous structure of actin (control conditions); broken arrows, loss of filamentous actin (stressed conditions). [Color figure can be viewed in the online issue, which is available at www.interscience.wiley.com.]

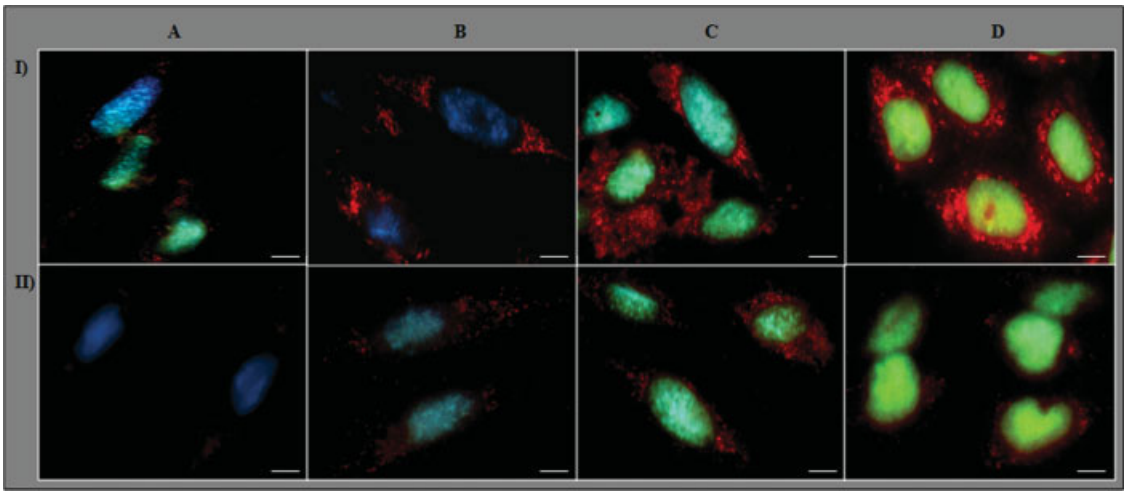

Fig. 7. Al-evoked ROS in the astrocytoma cell line. Cells were incubated in (**A**) control, (**B**) 0.01 mM Al, (**C**) 0.1 mM Al, and (**D**) 40 μM H_2O_2 for 24 hr. The cells were stained with Hoechst 33528 (nucleus) and DCFH-DA (ROS). **I:** A 24-hr incubation in control or stressed conditions. **II:** A 24-hr incubation in 1 mM NAC after exposure to control or stress conditions; a significant decrease in ROS after NAC treatment was evident. Microscopy was performed at 60× ocular objective; scale bar = 10 μm. Blue indicates nucleus; red, presence of ROS. Only minute amounts of ROS were detected in the control cells. [Color figure can be viewed in the online issue, which is available at www.interscience.wiley.com.]

argue against an apoptotic mechanism. We have previously observed that KG, like NAC, serves as a potent antioxidant reversing the toxic influence of Al (Mailloux et al., 2007b). Furthermore, the inactivation of α-ketoglutarate dehydrogenase observed in numerous disorders has been postulated to play an important role in KG homeostasis (Gibson et al., 2000). This moiety may help in the diminution of oxidative tension.

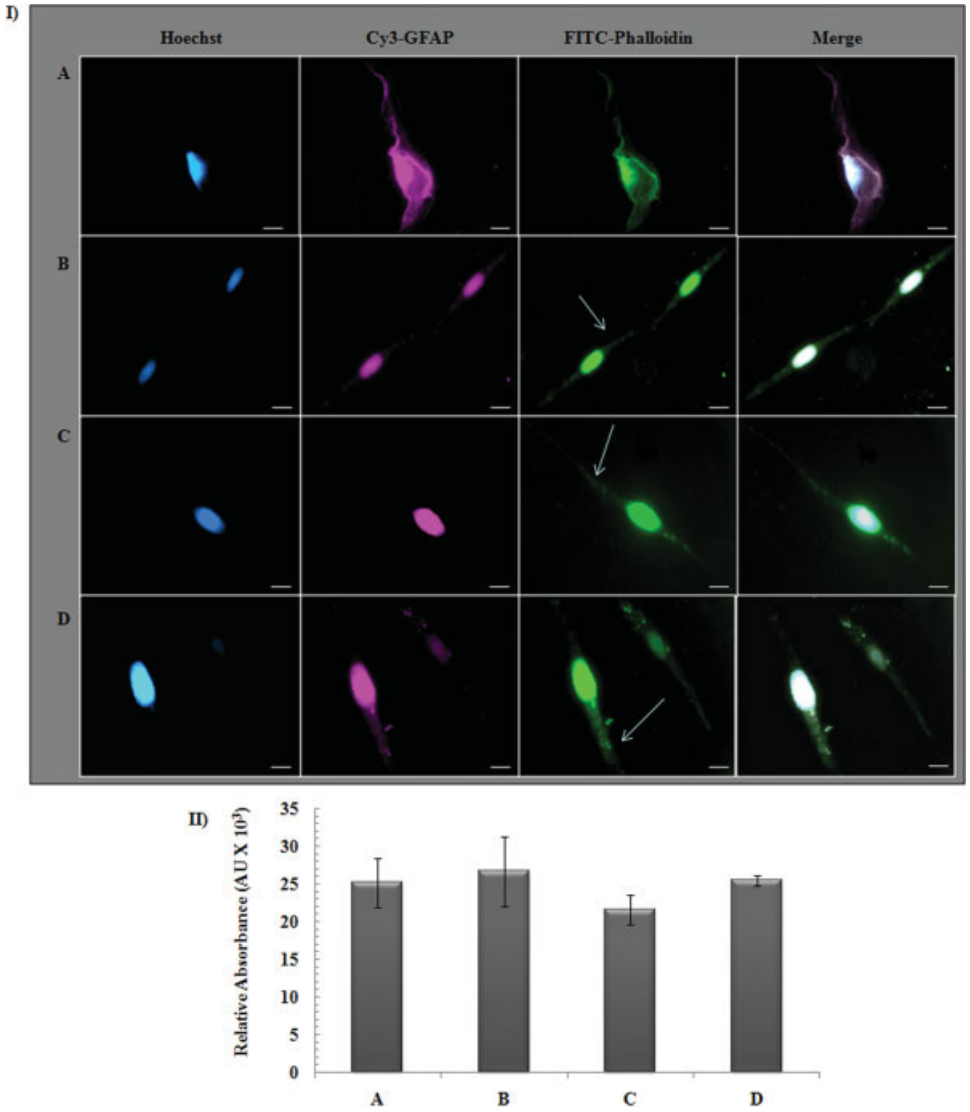

Fig. 8. Antioxidant treatment and the recovery of cytoskeletal architecture and energy status in human astrocytes (CCF-STTG1). **A:** Control cells. **B:** Cells treated with 0.01 mM Al. **C:** Cells exposed to 0.1 mM Al. **D:** Cells treated with 40 μM H_2O_2 for 24 hr. Cells were subsequently exposed to 1 mM NAC for 24 hr. **I:** Immunofluorescence staining with Hoechst 33528 (nucleus), Cy3-GFAP, and FITC-phalloidin (actin). Microscopy was performed at 40× ocular objective; scale bar = 10 μm. Arrows indicate the return of the filamentous structure of actin. **II:** HPLC analysis of cellular ATP levels. $n = 3 \pm SD$; $P \leq 0.05$. [Color figure can be viewed in the online issue, which is available at www.interscience.wiley.com.]

The Al-mediated disruption of the cytoskeleton via the depletion of cellular ATP was demonstrated further by reduced amount of profilin-2 in the astrocytoma cells. Previous work has shown that disruption of the mitochondrial membrane potential perturbs profilin expression (Clarkson et al., 2002). This low-molecular-weight protein is required to exchange ADP for ATP on globular actin monomers (Ackermann and Matus, 2003). The absence of profilin-2 significantly slows down actin polymerization (Paavilainen et al., 2004; Kovar et al., 2006). The enhanced production of ROS may also interfere with filament arrangements. These toxic molecules have been shown to disrupt cytoskeletal arrangements in various tissue types, including astrocytes (Zhu et al., 2005). Hence, it appears that the Al-mediated decrease in cellular ATP levels and the enhanced production of ROS disrupted the characteristic filamentous pattern of actin and GFAP in the human astrocytoma cells.

In the present study, cells treated with Al or H_2O_2 also displayed a sharp decrease in CK activity and expression. This situation would exacerbate the cellular depletion of energy because CK plays a key role in the homeostasis of ATP. The harmful effects of Al were compounded further by the severe reduction in the cellular levels of Cr and PCr. Intriguingly, CK in the control cells was predominantly associated with the actin filaments, a situation abolished after Al treatment. This observation suggests that CK may associate with the length of the actin filaments in order to produce ATP locally for the maintenance of the cytoskeletal structure and function. CK has been shown to associate with myofibrils to generate energy for skeletal and heart muscle contraction (Ventura-Clapier et al., 1994). Furthermore, glycolytic enzymes interact with polymerized actin, forming multienzyme complexes to produce ATP for cytoskeletal arrangements and organelle transport (Kraft et al., 2000). Hence, a dysfunctional ATP metabolism

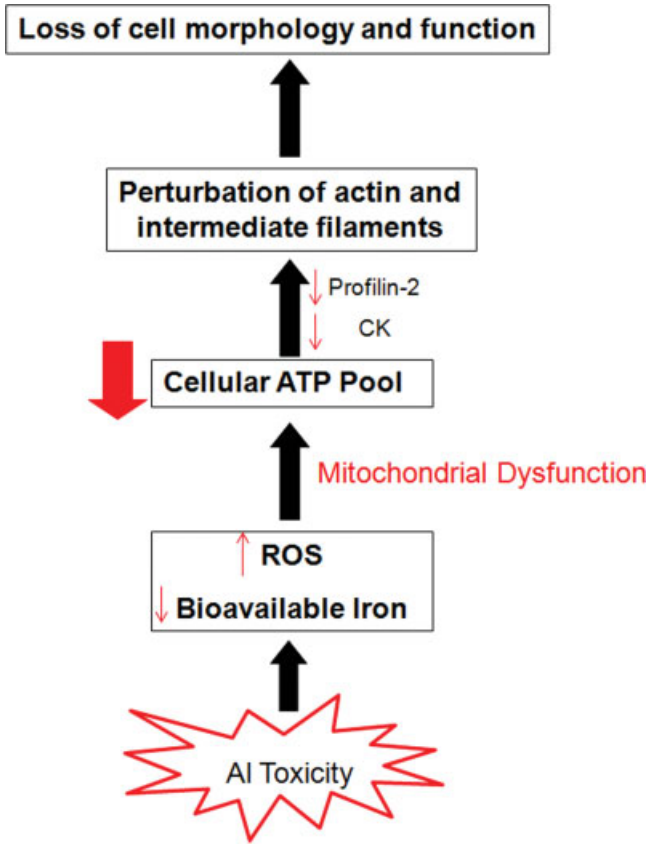

Fig. 9. Molecular link between Al toxicity and morphological perturbation in human astrocytoma cells. [Color figure can be viewed in the online issue, which is available at www.interscience.wiley.com.]

coupled with ineffective CK triggered by Al toxicity may have severe consequences for cerebral functions. The perturbation of polymerized actin and GFAP in astrocytes has been shown in patients with Alzheimer's disease (Tsuji and Shimohama, 2001). Intriguingly, astrocytes have also been shown to be the main site of Al accumulation in the human brain (Oshiro et al., 2000). Furthermore, recent work has revealed that neuronal death in Al-treated brain tissues only occurs after astrocyte dysfunction (Suarez-Fernandez et al., 1999). This study establishes an intimate connection between Al toxicity and astrocytic dysfunction. The ineffective oxidative ATP production culminates into abnormally shaped astrocytoma cells. It appears that the downstream ATP-requiring processes involved in maintaining cytoskeletal architecture are severely impeded.

This is the first demonstration of a molecular link between Al toxicity, perturbed cellular energy metabolism, and loss of cytoskeletal structure in human astrocytoma cells. Furthermore, these data also illustrate the important role CK plays in maintaining the energy budget needed to fuel the biochemical reactions responsible for maintaining cytoskeletal integrity. The Al-mediated disruption of cellular energy metabolism and the ensuing inability of CK and profilin-2 to fulfill their task manifests into the drastic morphological changes in the astrocytoma cells. This situation may portend dire consequences to the human brain and may explain the neurotoxicity of Al. Figure 9 illustrates a proposed relationship between Al toxicity, energy metabolism, and cytoskeletal structure.

ACKNOWLEDGMENT

Funding was received from the Northern Ontario Heritage Fund.

REFERENCES

Ackermann M, Matus A. 2003. Activity-induced targeting of profilin and stabilization of dendritic spine morphology. Nat Neurosci 6:1194–1200.

Ames A 3rd. 2000. CNS energy metabolism as related to function. Brain Res Brain Res Rev 34:42–68.

Anderson CM, Nedergaard M. 2003. Astrocyte-mediated control of cerebral microcirculation. Trends Neurosci 26:340–344.

Anderson CM, Swanson RA. 2000. Astrocyte glutamate transport: review of properties, regulation, and physiological functions. Glia 32:1–14.

Aremu DA, Meshitsuka S. 2006. Some aspects of astroglial functions and aluminum implications for neurodegeneration. Brain Res Rev 52:193–200.

Becaria A, Campbell A, Bondy SC. 2002. Aluminum as a toxicant. Toxicol Ind Health 18:309–320.

Bradford MM. 1976. A rapid and sensitive method for the quantitation of microgram quantities of protein utilizing the principle of protein-dye binding. Anal Biochem 72:248–254.

Clarkson MR, Murphy M, Gupta S, Lambe T, Mackenzie HS, Godson C, Martin F, Brady HR. 2002. High glucose-altered gene expression in mesangial cells. Actin-regulatory protein gene expression is triggered by oxidative stress and cytoskeletal disassembly. J Biol Chem 277:9707–9712.

Derouiche A, Anlauf E, Aumann G, Muhlstadt B, Lavialle M. 2002. Anatomical aspects of glia–synapse interaction: the perisynaptic glial sheath consists of a specialized astrocyte compartment. J Physiol Paris 96:177–182.

Dzeja PP, Terzic A. 2003. Phosphotransfer networks and cellular energetics. J Exp Biol 206(Pt 12):2039–2047.

Fink MP. 2002. Bench-to-bedside review: cytopathic hypoxia. Critical Care 6:491–499.

Gartlon J, Kinsner A, Bal-Price A, Coecke S, Clothier RH. 2006. Evaluation of a proposed in vitro test strategy using neuronal and non-neuronal cell systems for detecting neurotoxicity. Toxicol In Vitro 20:1569–1581.

Gibson GE, Park LC, Sheu KF, Blass JP, Calingasan NY. 2000. The alpha-ketoglutarate dehydrogenase complex in neurodegeneration. Neurochem Int 36:97–112.

Gourlay CW, Ayscough KR. 2005. The actin cytoskeleton: a key regulator of apoptosis and ageing? Nat Rev Mol Cell Biol 6:583–589.

Kovar DR, Harris ES, Mahaffy R, Higgs HN, Pollard TD. 2006. Control of the assembly of ATP- and ADP-actin by formins and profilin. Cell 124:423–435.

Kraft T, Hornemann T, Stolz M, Nier V, Wallimann T. 2000. Coupling of creatine kinase to glycolytic enzymes at the sarcomeric I-band of skeletal muscle: a biochemical study in situ. J Muscle Res Cell Motil 21:691–703.

Laemmli UK. 1970. Cleavage of structural proteins during the assembly of the head of bacteriophage T4. Nature 227(5259):680–685.

Leach RM, Hill HS, Snetkov VA, Ward JP. 2002. Hypoxia, energy state and pulmonary vasomotor tone. Respir Physiol Neurobiol 132:55–67.

Lemire J, Mailloux RJ, Appanna VD. 2008. Mitochondrial lactate dehydrogenase is involved in oxidative-energy metabolism in human astrocytoma cells (CCF-STTG1). PLoS ONE 3:e1550.

Mailloux R, Lemire J, Appanna V. 2007a. Aluminum-induced mitochondrial dysfunction leads to lipid accumulation in human hepatocytes: a link to obesity. Cell Physiol Biochem 20:627–638.

Mailloux RJ, Beriault R, Lemire J, Singh R, Chenier DR, Hamel RD, Appanna VD. 2007b. The tricarboxylic acid cycle, an ancient metabolic network with a novel twist. PLoS ONE 2:e690.

Mailloux RJ, Darwich R, Lemire J, Appanna V. 2008. The monitoring of nucleotide diphosphate kinase activity by blue native polyacrylamide gel electrophoresis. Electrophoresis 29:1484–1489.

Mentz S, de Lacalle S, Baerga-Ortiz A, Knauer MF, Knauer DJ, Komives EA. 1999. Mechanism of thrombin clearance by human astrocytoma cells. J Neurochem 72:980–987.

Oshiro S, Kawahara M, Kuroda Y, Zhang C, Cai Y, Kitajima S, Shirao M. 2000. Glial cells contribute more to iron and aluminum accumulation but are more resistant to oxidative stress than neuronal cells. Biochim Biophys Acta 1502:405–414.

Paavilainen VO, Bertling E, Falck S, Lappalainen P. 2004. Regulation of cytoskeletal dynamics by actin-monomer-binding proteins. Trends Cell Biol 14:386–394.

Pekny M, Nilsson M. 2005. Astrocyte activation and reactive gliosis. Glia 50:427–434.

Pessoa-Pureur R, Wajner M. 2007. Cytoskeleton as a potential target in the neuropathology of maple syrup urine disease: insight from animal studies. J Inherit Metab Dis 30:664–672.

Rutka JT, Murakami M, Dirks PB, Hubbard SL, Becker LE, Fukuyama K, Jung S, Tsugu A, Matsuzawa K. 1997. Role of glial filaments in cells and tumors of glial origin: a review. J Neurosurg 87:420–430.

Saks VA, Ventura-Clapier R, Aliev MK. 1996. Metabolic control and metabolic capacity: two aspects of creatine kinase functioning in the cells. Biochim Biophys Acta 1274:81–88.

Sauer U, Schlattner U. 2004. Inverse metabolic engineering with phosphagen kinase systems improves the cellular energy state. Metab Eng 6:220–228.

Schagger H, von Jagow G. 1991. Blue native electrophoresis for isolation of membrane protein complexes in enzymatically active form. Anal Biochem 199:223–231.

Singh R, Mailloux RJ, Puiseux-Dao S, Appanna VD. 2007. Oxidative stress evokes a metabolic adaptation that favors increased NADPH synthesis and decreased NADH production in Pseudomonas fluorescens. J Bacteriol 189:6665–6675.

Suarez-Fernandez MB, Soldado AB, Sanz-Medel A, Vega JA, Novelli A, Fernandez-Sanchez MT. 1999. Aluminum-induced degeneration of astrocytes occurs via apoptosis and results in neuronal death. Brain Res 835:125–136.

Ting KK, Brew B, Guillemin G. 2007. The involvement of astrocytes and kynurenine pathway in Alzheimer's disease. Neurotox Res 12:247–262.

Tsuji T, Shimohama S. 2001. Analysis of the proteomic profiling of brain tissue in Alzheimer's disease. Dis Markers 17:247–257.

Ventura-Clapier R, Veksler V, Hoerter JA. 1994. Myofibrillar creatine kinase and cardiac contraction. Mol Cell Biochem 133–134:125–144.

Wieser W, Krumschnabel G. 2001. Hierarchies of ATP-consuming processes: direct compared with indirect measurements, and comparative aspects. Biochem J 355(Pt 2):389–395.

Yoshida M, Muneyuki E, Hisabori T. 2001. ATP synthase—a marvellous rotary engine of the cell. Nat Rev Mol Cell Biol 2:669–677.

Zhu D, Tan KS, Zhang X, Sun AY, Sun GY, Lee JC. 2005. Hydrogen peroxide alters membrane and cytoskeleton properties and increases intercellular connections in astrocytes. J Cell Sci 118(Pt 16):3695–3703.